Journal of Atmospheric and Solar-Terrestrial Physics 105-106 (2013) 308–312

Contents lists available at ScienceDirect

Journal of Atmospheric and Solar-Terrestrial Physics

journal homepage: www.elsevier.com/locate/jastp

# Optical and radar observations of small-scale polar cap auroral structures

M. Samara *, R.G. Michell

*Southwest Research Institute, San Antonio, TX, United States*

A R T I C L E  I N F O

*Article history:*
Received 8 April 2012
Received in revised form
22 November 2012
Accepted 26 November 2012
Available online 16 December 2012

*Keywords:*
Aurora
Imaging
Incoherent Scatter Radar
RISR
Polar cap

A B S T R A C T

We present ground-based auroral observations from Resolute Bay, Nunavut, Canada (74.73°N, 94.9°W) during January 2011. Two electron-multiplying CCD (EMCCD) imagers were operated at 31 frames per second. One was equipped with an all-sky field of view (FOV) lens and the other with a narrow (19°) FOV lens, centered on the geographic zenith (0° Az., 90° El.), a few degrees away from magnetic zenith (315° Az., 88° El.). The Resolute Incoherent Scatter Radar (RISR) was operating in a mode that enabled common-volume observations with the imagers. Being well inside the polar cap, the magnetic field at Resolute Bay is considered 'open' and connects to the lobes of the magnetotail. However, there is no clear consensus on whether polar cap aurorae occur on open or closed field lines. The electron acceleration is likely driven by direct solar wind processes, distant tail lobe processes or plasma sheet processes. One possible mechanism for accelerating the precipitating electrons is the parallel electric field of inertial Alfvén waves. The dynamic nature of the small-scale auroral features, observed on several nights, and the altitude extent of the ionization observed with RISR provide support for this hypothesis.



## 1. Introduction and background

Polar cap aurorae have been observed for decades, with the first reported observations occurring in the early 20th century (Mawson and Chree, 1925). During the international geophysical year of 1958–1959 the study of polar cap aurora increased significantly due to the advent of the all-sky camera (Davis, 1960). The full history and recent state of polar cap auroral observations is summarized in the review by Zhu et al. (1997).

The statistical dependence of polar cap aurorae on the interplanetary magnetic field (IMF) is a subject of debate. Studies have been done using both ground-based and satellite data (Zhu et al., 1997). Ground-based imaging is better suited for the study of the fainter, smaller scale auroral arcs, while satellite instrumentation for observing the brighter, large scale aurora. There are likely multiple types of polar cap aurorae with varying levels of brightness and scale size and this may be why there have been disparities in reporting. A correlation between polar cap aurora and IMF $B_y$ has been deduced from satellite optical observations. Imaging from the Defense Meteorological Satellite Program (DMSP) in visible wavelengths and Viking UV observations has shown that the polar cap aurora is preferentially seen in the morning sector for IMF $B_y$ negative and the evening sector for IMF $B_y$ positive (Gussenhoven, 1982; Elphinstone et al., 1990; Makita et al., 1991; Kullen et al., 2002). Ground-based studies have not yielded this particular correlation but instead one between the dawn-dusk motion of the auroral structures and the direction of the IMF $B_y$ (Rairden and Mende, 1989; Valladares et al., 1994).

More recently, Cumnock et al. (2009) used a combination of polar UVI and DMSP electron data to examine the IMF dependence of large-scale polar cap auroral arcs, which show substructure in the particle signatures. They found a correlation between the occurrence of polar cap aurora and northward IMF followed by a change in IMF $B_y$. In addition, Kullen et al. (2002) found no IMF correlation between the less-common midnight and multiple arc events.

The ion and electron signatures of bright polar cap aurora are similar to those found in the auroral oval and therefore it is assumed that the bright polar cap auroral arcs also have a plasma sheet source population, consistent with a region of closed field lines extending up into the polar cap (Meng, 1981). There is still no clear consensus on whether all polar cap aurorae occur on open or closed field lines or if some occur on open and some on closed field lines. Conjugate satellite observations of polar cap arcs (Obara et al., 1988; Huang et al., 1989) have provided evidence that they occur on closed field lines. Bonnell et al. (1999) found, using data from the Fast Auroral SnapshoT (FAST) satellite, that the lobe reconnection model was consistent with

* Corresponding author. Tel.: +1 210 522 6066.
*E-mail address:* msamara@swri.edu (M. Samara).

1364-6826/$ - see front matter © 2012 Elsevier Ltd. All rights reserved.
http://dx.doi.org/10.1016/j.jastp.2012.11.016

the electrodynamics and temperatures of the precipitating electrons and ions, but not the presence of precipitating $O^+$, which was observed. The plasma sheet source model was consistent with the composition, but not the temperature of the observed precipitating electrons and ions.

It should be noted that these previous studies used satellite imagery to identify polar cap arcs, and were therefore selecting for large-scale and long-lived auroral features. The large-scale features are most often a northward IMF phenomenon. The high time-cadence ground-based imagers used in this study enabled the observation of small-scale and transient auroral structures that occur inside the polar cap, which show less correlation to IMF conditions.

## 2. Method

An observational campaign was conducted from Resolute Bay, Nunavut, Canada, at a geodetic location of 74.7°N, 94.9°W (82.5°N, 52.4°W geomagnetic) with local magnetic midnight occurring at approximately 07:45 UT. The optical data were recorded using two electron-multiplying CCD (EMCCD) imagers, both unfiltered, recording the white-light auroral emissions at 31 frames per second. One was equipped with an all-sky field of view (FOV) lens and the other with a narrow field of view (FOV) lens (19°). The spatial resolution is approximately 1.5 pixels per degree, or 800 m–1 km per pixel in the vicinity of the zenith for the all-sky imager and approximately 13 pixels per degree, or 100 m per pixel for the narrow field imager.

The campaign was conducted in early January, from the 7th to the 18th, in order to maximize the local time coverage of the potential auroral observations. The RISR radar operated nearly continuously during that time interval and auroral structures were observed in the optics on several nights when clear observing conditions existed.

## 3. Observations

The nights of 8 and 9 January 2011 had good observing conditions with few clouds and blowing snow. The resolute incoherent scatter radar (RISR) was running a long plulse (480 μs) raw data mode with multiple beam positions, including one up the geographic zenith (26.6° Az., 90.0° El.) which is very close to magnetic zenith (315° Az., 88° El.). The magnetic zenith is the best place to observe the altitude profiles of ionization resulting from auroral particle precipitation with the radar and also to distinguish the perpendicular widths of auroral structures observed in the images. If one looks off-zenith the altitude extent of the aurora cannot be distinguished from the horizontal extent.

### 3.1. 8 January 2011

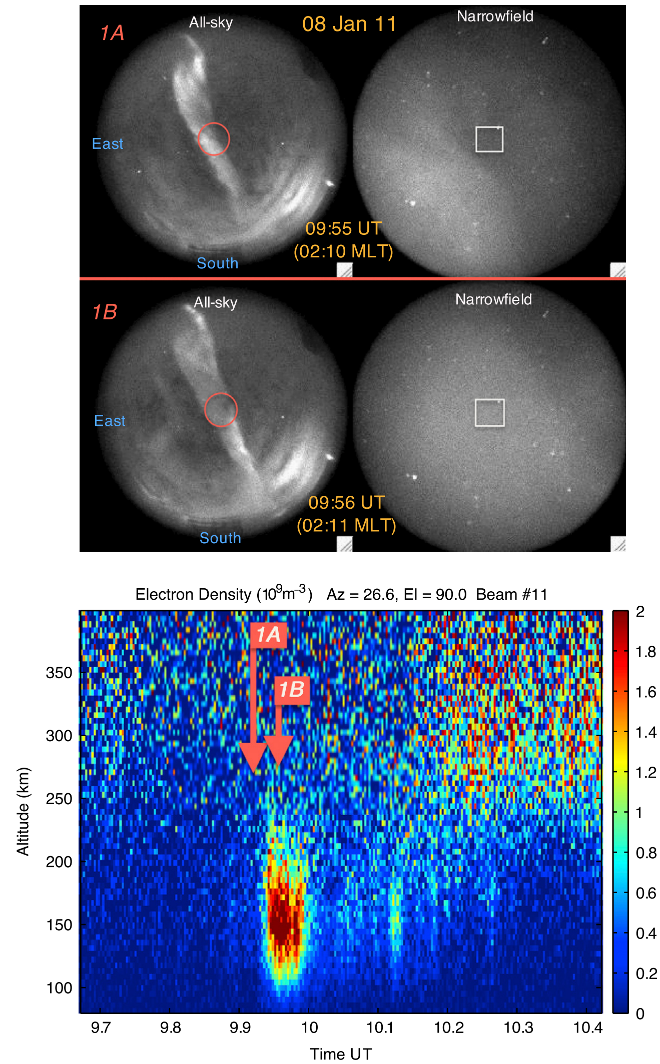


**Fig. 1.** All-sky (left), corresponding narrowfield image (right) and electron density (bottom) for a bright North-South aligned auroral arc passing over Resolute Bay on 8 January 2011. (A) At 09:55 UT (02:10 MLT) and (B) at 09:56 UT (02:11 MLT). North is at the top and East is to the left. The electron density profiles cover ~50 min near 10:00 UT and the color scale is $\times 10^9$ m$^{-3}$.

Fig. 1 shows auroral images from both the all-sky (left) and narrowfield (right) imagers at 09:55 UT (top) and 09:56 UT (bottom), at 02:10 MLT and 02:11 MLT respectively. In these views, North is at the top and East is to the left. This particular auroral arc occurred in the midnight sector and was the brightest and the only one observed to be mostly North-South aligned during the campaign. It formed quickly, with an arc width in the E–W direction of approximately 10–20 km, and lasted for only 15 min before dissipating. The RISR electron density enhancement associated with this auroral arc is shown at the bottom. These data cover a time period of approximately 50 min near 10:00 UT. The electron density enhancement lasted 5 min, which corresponds to the time it took for the auroral arc to pass through the zenith.

The long pulse of the radar (480 μs) corresponds to approximately 72 km of range smearing. Thus, accurate determinations of the altitude of the electron density enhancements cannot be made. In this example, the approximate altitude of the peak auroral ionization is 150 km, which is higher than what is typically observed for aurora in the oval (110–140 km) with the same long pulse. Using the simple model of Rees (1963), 150 km altitude corresponds to precipitating electrons with a characteristic energy of ~1−2 keV, which is indeed lower than that typically observed in the auroral oval. The enhanced ionization extends from near 100 km to 225 km in altitude, indicating that there is a large range of electron energies present in the precipitating population.

At a later time on that same night a mostly East-West aligned arc was observed, near 16:07 UT (08:22 MLT), in the morning sector. Fig. 2 is an all-sky image of this thin auroral arc structure that formed just before sunrise which was approximately 5 km wide and lasted for approximately 5 min. The bright portion on the left is the sunrise, hence the imager saturated. While the arc

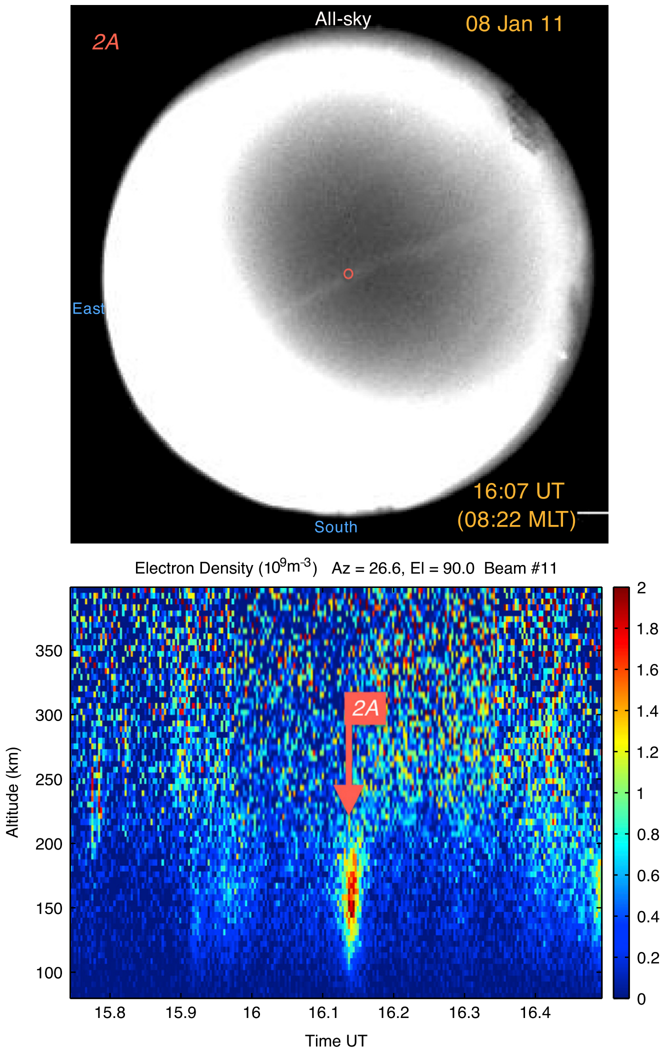


Fig. 2. All-sky image of a thin E–W aligned auroral arc over Resolute Bay on 8 January 2011, near 16:07 UT (08:22 MLT). North is at the top and East is to the left. The electron density profiles cover ~40 min around 16:00 UT and the color scale is $\times 10^9\ m^{-3}$.

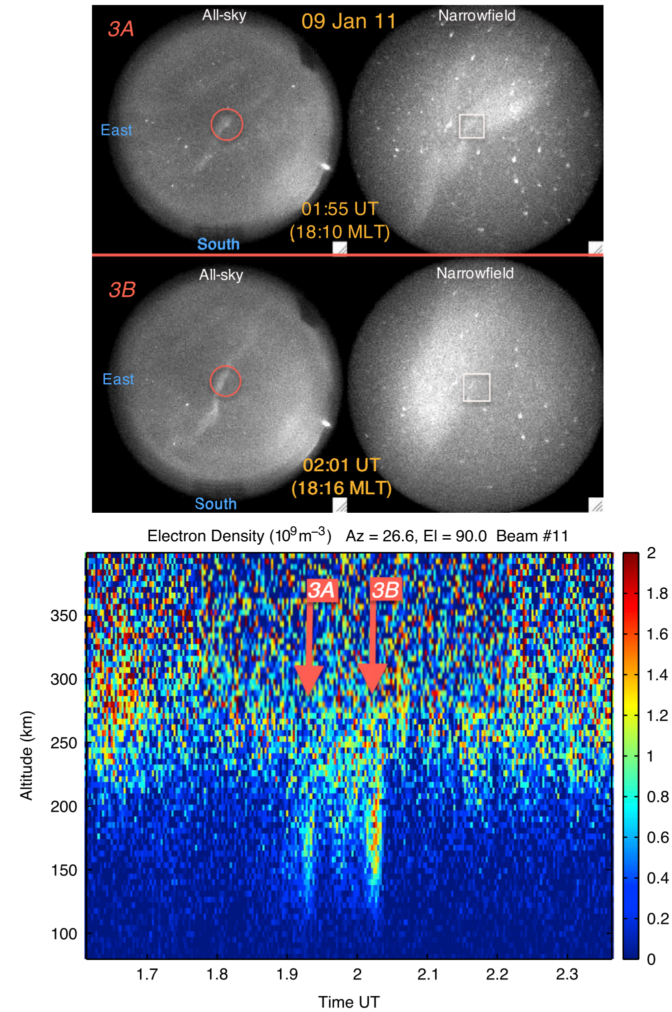


Fig. 3. All-sky (left), corresponding narrowfield image (right) and electron density (bottom) for two narrow auroral arcs that passed through the zenith over Resolute Bay on 9 January 2011. (A) At 01:55 UT (18:10 MLT) and (B) at 02:01 UT (18:16 MLT). North is at the top and East is to the left. The electron density profiles cover ~45 min around 02:00 UT and the color scale is $\times 10^9\ m^{-3}$.

can also be seen in the narrowfield it was nearly saturated as well resulting in inadequate contrast for clearly seeing the arc in any one image. The corresponding RISR electron density profiles, covering approximately 40 min near 16:00 UT, are shown at the bottom. The altitude profile of the ionization is similar to the N–S arc, although in this case the ionization does not extend as low in altitude, indicating less electrons with energies greater than 5 keV.

### 3.2. 9 January 2011

The following night (9 January 2011), auroral structures were again visible in the zenith near 02:00 UT (18:15 MLT). Fig. 3 is in the same format as Fig. 1. The two sets of images were taken 6 min apart and correspond to two separate thin auroral arc structures that passed through the zenith. The top row was taken at 01:55 UT (18:10 MLT) and the bottom one at 02:01UT (18:16 MLT). The all-sky images (left) show the general South-East to North-West alignment of these arcs. These auroral structures occurred in the evening sector and the widths of the small-scale features were in the 1–5 km range. The associated electron density enhancement is similar to that for the morning side aurora on the previous night, extending from ~125 km to 225 km in altitude. Enhancements in the F-region electron density, that were not correlated with any auroral structures, were observed.

The last example shows the most structured and dynamic aurora which occurred later on 9 January 2011, near 12:39 UT (04:54 MLT). Fig. 4 shows one set of auroral images from both all-sky and narrowfield imagers. This auroral arc structure contained highly variable structure as it passed through the zenith. The narrowfield images show curl-like motions of ~ kilometer scale auroral features. The auroral density enhancement associated with this last case is again very similar to the other three cases. The altitude extends from ~125 km to 200 km and appears to occur just before an F-region density enhancement. The enhanced F-region density can be seen to start just after the aurora passed through the zenith.

## 4. Discussion

These auroral observations span a range of local times, covering dusk, post midnight, dawn and morning side, and a range of

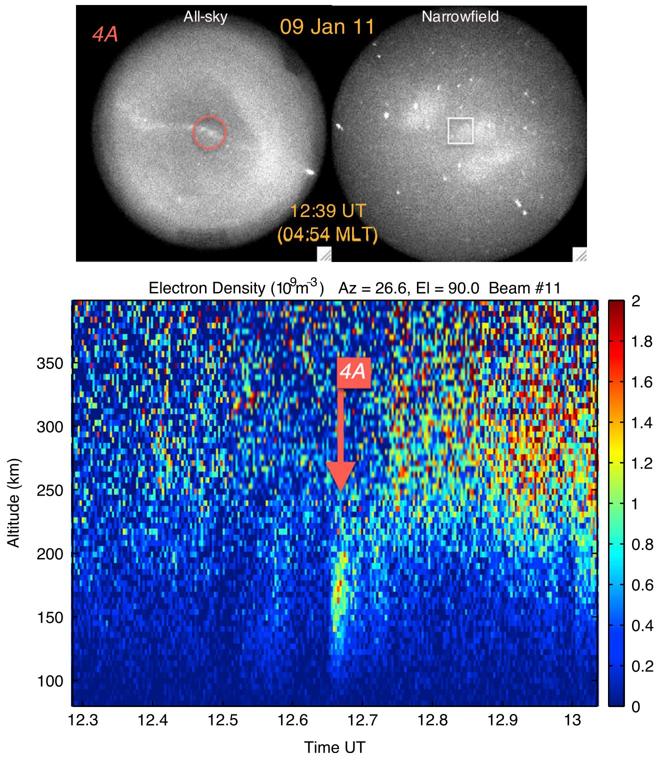


**Fig. 4.** All-sky (left), corresponding narrowfield image (right) and electron density (bottom) for a narrow, highly structured auroral arc that passed through the zenith over Resolute Bay on 9 January 2011, near 12:39 UT (04:54 MLT). North is at the top and East is to the left. The electron density profiles cover $\sim 45$ min around 12:30 UT and the color scale is $\times 10^9$ m$^{-3}$.

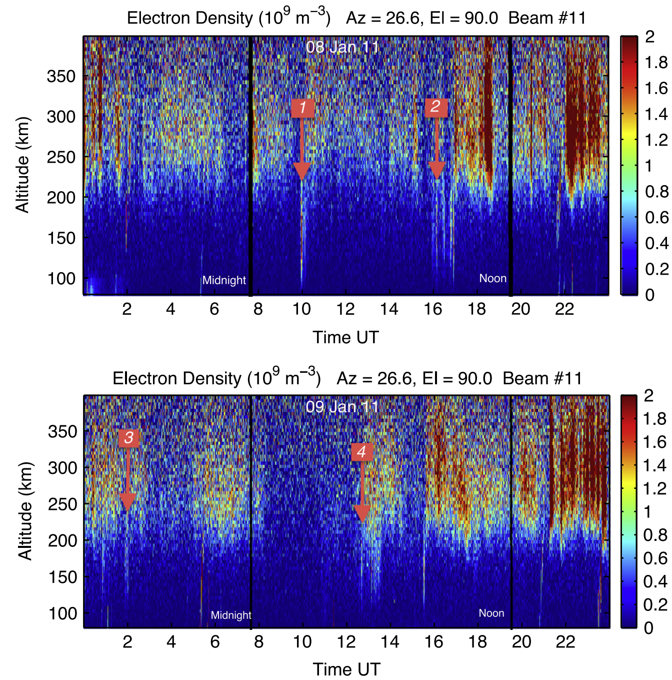


**Fig. 5.** RISR electron density profiles for 8 January 2011, covering a time period of 24 h. The color scale is $\times$ $10^9$ m$^{-3}$. Local magnetic midnight is at 07:45 UT and local noon is at 19:45 UT. Noon and midnight are denoted by black vertical lines.

different types of auroral structures. In all cases the auroral arcs were fairly thin ($\leq 20$ km) in the direction perpendicular to the magnetic field, and contained motion of small-scale ($\sim 1$ km) features inside the main auroral arc. The combination of imaging and incoherent scatter radar produces a complimentary view in terms of the ionization profile and the ionospheric context. The density profile and altitude of peak ionization can be used to estimate the characteristic energy of the precipitating electron spectrum. According to the simple model of Rees (1963), these polar cap auroral structures correspond to electron energies in the approximate range of 200 eV–2 keV. This range is lower than typically observed in the auroral zone and likely reflects the differing acceleration mechanism at work in the polar cap, although inertial Alfvén wave acceleration has been shown to be effective at accelerating electrons to these energies in the auroral zone (Chaston et al., 2003).

The RISR electron density data, presented in Fig. 5 for both 8 and 9 January 2011, show more structure and variation in the F-region plasma (250–350 km altitude) than the E-region plasma (below 200 km altitude). The scale is the same as in the previous figures, but here the F-region variations are clearly visible. These variations are potentially the result of higher density plasma convecting into the polar cap from lower latitudes. The auroral density enhancements can be seen near 10 and 16 UT. The arcs occurred near the boundaries or edges of F-region enhancements. This is consistent with the hypothesis that polar cap aurorae occur on boundaries and flow shear gradients in the ionospheric convection pattern (Reiff et al., 1978; Lyons, 1985; Sandholt et al., 2006).

There is no clear correlation with the solar wind IMF for either 8 or 9 January 2011. The geomagnetic conditions throughout this time period were quiet, with a $K_p$ of between 2 and 3. The three components of the IMF showed large variability, with $B_z$ nearly zero, $B_x$ $\sim 2-3$ nT North and $B_y$ $\sim 2-3$ nT South. The solar wind speed was relatively high during this time (between 500 and 600 km/s), consistent with the observations of Kullen et al. (2002), although the IMF magnitude was small, only $\sim 5$ nT.

In the review by Zhu et al. (1997), several different source and generator models are discussed as there are likely multiple acceleration processes that produce polar cap auroral arcs. For example, large-scale magnetospheric dynamics driven by Northward IMF can produce large-scale polar cap auroral arcs (Lassen and Danielsen, 1978), such as the 'Theta-aurora' (Frank et al., 1986). Small-scale polar cap auroral arcs are likely generated by more localized processes, such as inertial Alfvén wave acceleration or plasma density and pressure gradients in the convection over the polar cap.

The small-scale auroral features in the polar cap, present in all the examples shown here, provide evidence for determining the possible acceleration mechanisms through their altitude extent and ionization profiles. The small-scale ($\sim 1$ km) dynamic manifestation of the auroral structures and their faint (nearly sub-visual) nature are consistent with acceleration by inertial Alfvén waves, as predicted by Chaston et al. (2003). The auroral image data were taken in white-light (unfiltered) and therefore absolute intensity values cannot be assigned. Future studies will use narrowband filters to quantify the auroral intensity in Rayleighs, enabling further insight into acceleration mechanisms and comparisons to theory.

## 5. Conclusion

Polar cap arcs and especially their smaller scale features are likely the result of electrons that have been accelerated by inertial Alfvén waves. The imaging observations presented here show the dynamic, small-scale nature of the auroral features. The RISR data reveal that the energy of the precipitating electrons is consistent with the energies expected from Alfvén wave acceleration.

Moreover, the auroral arcs were found to occur near the boundaries of the F-region plasma enhancements which is consistent with the expectation that arcs would form in the regions where currents would be flowing. These observations verify the existence of dynamic, small-scale ($\sim 1$ km) auroral features in the polar cap and the need for high-resolution narrow FOV auroral imaging observations for better understanding the acceleration processes and source plasma regions.

## Acknowledgments

The authors would like to thank SRI International, particularly Craig Heinselman for arranging the radar mode, Perry Morine for operating the radar and Shelly Easterday for assisting in the logistics of our stay at Resolute Bay. This work was supported by an Internal Research Grant from the Advisory Committee for Research at Southwest Research Institute, with partial support from NSF under Grant AGS-1139135.

## References

Bonnell, J., Elphic, R.C., Palfery, S., Strangeway, R.J., Peterson, W.K., Klumpar, D., Carlson, C.W., Ergun, R.E., McFadden, J.P., 1999. Observations of polar cap arcs on FAST. Journal of Geophysical Research 104, 12669–12682.

Chaston, C.C., Peticolas, L.M., Bonnell, J.W., Carlson, C.W., Ergun, R.E., McFadden, J.P., Strangeway, R.J., 2003. Width and brightness of auroral arcs driven by inertial Alfven waves. Journal of Geophysical Research (Space Physics) 108, 1091.

Cumnock, J.A., Blomberg, L.G., Kullen, A., Karlsson, T., Sundberg, K.Â.T., 2009. Small-scale characteristics of extremely high latitude aurora. Annales Geophysicae 27, 3335–3347.

Davis, T.N., 1960. The morphology of the polar aurora. Journal of Geophysical Research 65, 3497.

Elphinstone, R.D., Jankowska, K., Murphree, J.S., Cogger, L.L., 1990. The configuration of the auroral distribution for interplanetary magnetic field Bz northward. I: IMF Bx and By dependencies as observed by the Viking satellite. Journal of Geophysical Research 95, 5791–5804.

Frank, L.A., Craven, J.D., Gurnett, D.A., Shawhan, S.D., Burch, J.L., Winningham, J.D., Chappell, C.R., Waite, J.H., Maynard, N.C., Sugiura, M., 1986. The theta aurora. Journal of Geophysical Research 91, 3177–3224.

Gussenhoven, M.S., 1982. Extremely high latitude auroras. Journal of Geophysical Research 87, 2401–2412.

Huang, C.Y., Craven, J.D., Frank, L.A., 1989. Simultaneous observations of a theta aurora and associated magnetotail plasmas. Journal of Geophysical Research 94, 10137–10143.

Kullen, A., Brittnacher, M., Cumnock, J.A., Blomberg, L.G., 2002. Solar wind dependence of the occurrence and motion of polar auroral arcs: a statistical study. Journal of Geophysical Research 107, 1362.

Lassen, K., Danielsen, C., 1978. Quiet time pattern of auroral arcs for different directions of the interplanetary magnetic field in the *Y–Z* plane. Journal of Geophysical Research 83, 5277–5284.

Lyons, L.R., 1985. A simple model for polar cap convection patterns and generation of theta auroras. Journal of Geophysical Research 90, 1561–1567.

Makita, K., Meng, C.I., Akasofu, S.I., 1991. Transpolar auroras, their particle 245 precipitation, and IMF B(y) component. Journal of Geophysical Research 96, 14085.

Mawson, D., Chree, C., 1925. Records of the aurora polaris. In: Magnetism and Aurora, vol. 2, A.J. Kent, Sydney, Australia, Govt. Printer.

Meng, C.I., 1981. Polar cap arcs and the plasma sheet. Geophysical Research Letters 8, 273–276.

Obara, T., Kitayama, M., Mukai, T., Kaya, N., Murphree, J.S., 1988. Simultaneous observations of sun-aligned polar CAP arcs in both hemispheres by EXOS-C and Viking. Geophysical Research Letters 15, 713–716.

Rairden, R.L., Mende, S.B., 1989. Properties of 6300-A auroral emissions at South Pole. Journal of Geophysical Research 94, 1402–1416.

Rees, M.H., 1963. Auroral ionization and excitation by incident energetic electrons. Planetary and Space Science 11, 1209.

Reiff, P.H., Burch, J.L., Heelis, R.A., 1978. Dayside auroral arcs and convection. Geophysical Research Letters 5, 391–394.

Sandholt, P.E., Dyrland, M., Farrugia, C.J., 2006. Dayside aurorae and polar arcs under south-east IMF orientation. Annales Geophysicae 24, 3421–3432.

Valladares, C.E., Carlson Jr., H.C., Fukui, K., 1994. Interplanetary magnetic field dependency of stable Sun-aligned polar cap arcs. Journal of Geophysical Research 99, 6247–6272.

Zhu, L., Schunk, R.W., Sojka, J.J., 1997. Polar cap arcs: a review. Journal of Atmospheric and Solar–Terrestrial Physics 59, 1087–1126.